[4+3] versus [4+2] Mechanisms in the Dimerization of 2-Boryl-1,3-butadienes. A Theoretical and Experimental Study

François Carreaux,*,[†] Françoise Possémé,[†] Bertrand Carboni,[†] Ana Arrieta,[‡]
Begoña Lecea,[§] and Fernando P. Cossío*,[‡]

*Synthèse et Electrosynthèse Organiques, Institut de Chimie, UMR CNRS 6510, Avenue du Général
Leclerc, F35042, Rennes Cedex, France, Kimika Fakultatea, Euskal Herriko Unibertsitatea, P. K. 1072,
20080 San Sebastián-Donostia, Spain, and Farmazi Fakultatea, Euskal Herriko Unibertsitatea,
P. K. 450, 01080 Vitoria-Gasteiz, Spain*

qopcomof@sq.ehu.es

Received September 29, 2002

The thermal dimerization of 2-boryl-1,3-butadienes and the scope of this reaction to prepare six-membered rings difficult to synthesize by other methodologies have been studied. In addition, the nature of this dimerization has been studied theoretically. It has been found that the reaction coordinate associated with the formation of the cycloadduct of lowest energy has significant [4+3] character. This behavior is caused by the favorable carbon−carbon overlap and the large values of the corresponding resonance integrals. However, beyond the transition structure, the [4+2] pathway becomes the preferred one thus leading to the exclusive formation of the [4+2] cycloadduct. Aside from this effect, donating groups at the boryl moiety favor the [4+2] mechanism.

Introduction

The use of Diels−Alder reactions is one of the most commonly encountered strategies for the formation of six-membered rings, particularly in natural product synthesis.[1] The scope of this reaction has been further augmented by using synthetic equivalents of either the diene or the dienophile. For instance, alkenylboron dienophiles have been used as synthetic equivalents of enols and enamines.[2,3] Recent reports from this laboratory and others have detailed the exceptional and unusual characteristics of Diels−Alder reactions of 1,3-dienyl-2-boronates.[4] The pinacol ester of (1,3-butadien-2-yl)boronic acid **1** (Scheme 1, $R_2 = -O\text{-CMe}_2\text{-CMe}_2\text{-O}-$) is found to be a reactive diene for the Diels−Alder reaction to produce functionalized cyclic 1-alkenylboronates in high yields. However, **1** is also highly susceptible to dimerize to give **2**, even at room temperature, as its ester or sulfone congeners.[5] Although the high propensity of **1** toward Diels−Alder dimerization has been known for some time,[4a] no experimental and theoretical study of this

SCHEME 1[a]
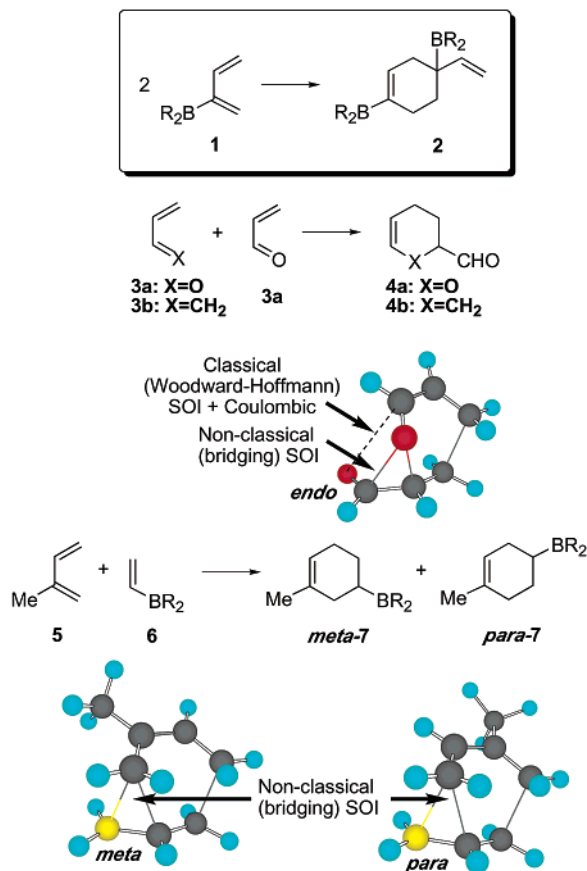
[a] SOI stands for secondary orbital interaction.

process has been reported up to now. Considering the synthetic potential of **2**, which possesses both vinyl and

[†] Institut de Chimie.
[‡] Kimika Fakultatea.
[§] Farmazi Fakultatea.

(1) For a review on intermolecular Diels−Alder reactions, see: Oppolzer, W. In *Comprehensive Organic Synthesis*; Trost, B. M., Fleming, I., Paquette, L. A., Eds.; Pergamon: Oxford, UK, 1991; Vol. 5, pp 315−399.

(2) For the first example of the use of an organoboron compound in an intermolecular Diels−Alder reaction, see: Matteson, D. S.; Waldbillig, J. O. *J. Org. Chem.* **1963**, *28*, 366.

(3) For examples of the use of alkenylboron compounds as dienophiles in intermolecular Diels−Alder reactions see: Singleton, D. A.; Lee, Y.-K. In *Advances in cycloaddition*; Lautens, M., Ed.; JAI Press: Greenwich, CT, 1997; Vol. 4, pp 121−148.

(4) (a) Guennouni, N.; Rasset-Deloge, C.; Carboni, B.; Vaultier, M. *Synlett* **1992**, 581. (b) Kamabuchi, A.; Miyaura, N.; Suzuki, A. *Tetrahedron Lett.* **1993**, *34*, 4827. (c) Renaud, J.; Graf, C.-D.; Oberer, L. *Angew. Chem., Int. Ed.* **2000**, *39*, 3101.

alkyl boronic moieties, we decided to offer a rationalization of this phenomenon.
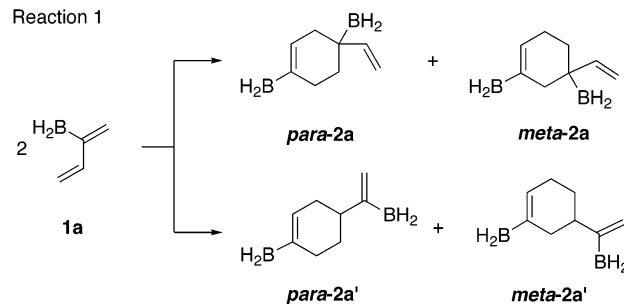
Aside from the preparative utility of this reaction, the nature of its mechanism is very interesting in a wider context. Thus, the well-known dimerization of acrolein **3** has been used as a textbook case to show the importance of second-order orbital interactions.[6] A recent paper from Quadrelli et al.[7] on the 2 **3a** → **4a** transformation has shown the importance of nonclassical (bridging) and classical (Woodward–Hoffmann[8]) secondary orbital interactions in the formation of the 2-substituted dimer **4a** as indicated in Scheme 1. In addition, a detailed study by Evanseck and Kong[9] on the Diels–Alder reaction between acrolein and butadiene (Scheme 1, **3a** + **3b** → **4b**) has shown that the nonclassical [4+3] term is the most important one among the possible secondary orbital interactions, and that this effect is increased when solvent effects are taken into account.

The different regioselectivities observed in the reaction between dienes **5** and vinyl boranes **6** (Scheme 1) have been widely studied by Singleton.[10] This author and, recently, Goodman et al.[11] have found that, although the [4+2] cycloadducts are formed in the **5** + **6** → **7** transformation, the geometries of the corresponding transition structures are compatible with [4+3] interactions, favoring the formation of the meta-cycloadducts **7** indicated in Scheme 1. In this latter case these nonclassical (bridging) secondary orbital interactions involving B···C terms have been detected computationally. However, the reasons underlying the final exclusive formation of [4+2] cycloadducts are not clear at present. In addition, the validity (or the necessity) of the secondary orbital interactions model has been questioned[12] and direct measurement of the magnitude of this kind of interaction is required[9,13] to assess the validity of the model.
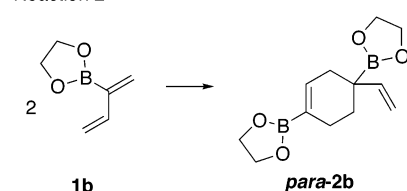
Within this context, the present work aims to explore the scope of the **1** + **1** → **2** transformation and subsequent reactions to yield cyclic structures not readily accessible by conventional hydroboration techniques. In addition, in this paper we report for the first time a computational study of the mechanism of this particular transformation, as well as a direct evaluation of the nonclassical secondary orbital interactions. Finally, an explanation for the evolution from [4+3] to [4+2] structures is presented.

(5) (a) McIntosh, J. M.; Sieler, R. A. *J. Org. Chem.* **1978**, *43*, 4431. (b) Hoffmann, H. M. R.; Weichert, A.; Slawin, A. M. Z.; Williams, D. J. *Tetrahedron* **1990**, *46*, 5591.

(6) Fleming, I. *Frontier Orbitals and Organic Chemical Reactions*; Wiley: New York, 1976; p 141.

(7) Toma, L.; Quadrelli, P.; Caramella, P. *Tetrahedron Lett.* **2001**, *42*, 731.

(8) Hoffmann, R.; Woodward, R. B. *J. Am. Chem. Soc.* **1965**, *87*, 4388.

(9) Kong, S.; Evanseck, J. D. *J. Am. Chem. Soc.* **2000**, *122*, 10418.

(10) (a) Singleton, D. A. *J. Am. Chem. Soc.* **1992**, *114*, 6563. (b) Singleton, D. A.; Martinez, J. P. *J. Am. Chem. Soc.* **1990**, *112*, 7423. (c) Singleton, D. A.; Martinez, J. P. *Tetrahedron Lett.* **1991**, *32*, 7365. (d) Singleton, D. A.; Martinez, J. P.; Watson, J. V. *Tetrahedron Lett.* **1992**, *33*, 1017. (e) Singleton, D. A.; Martinez, J. P.; Ndip, G. M. *J. Org. Chem.* **1992**, *57*, 5768. (f) Singleton, D. A.; Martinez, J. P.; Watson, J. V.; Ndip, G. M. *Tetrahedron* **1992**, *48*, 5831.

(11) Pellegrinet, S. C.; Silva, M. A.; Goodman, J. M. *J. Am. Chem. Soc.* **2001**, *123*, 8832.

(12) García, J. I.; Mayoral, J. A.; Salvatella, L. *Acc. Chem. Res.* **2000**, *33*, 658.

(13) Arrieta, A.; Cossío, F. P.; Lecea, B. *J. Org. Chem.* **2001**, *66*, 6178.

SCHEME 2

Reaction 1

Reaction 2

Computational Methods

All calculations included in this paper have been obtained by using the GAUSSIAN 98[14] series of programs, with the standard 6-31+G* basis set.[15] To include electron correlation at a reasonable computational cost, Density Functional Theory (DFT)[16] has been used. In this study, these calculations have been carried out by means of the three-parameter functional developed by Becke,[17] which is usually denoted as B3LYP. This method has been shown to produce reliable results in pericyclic rections and, in particular, in [4+2] cycloadditions.[18] Zero-point vibrational energies (ZPVEs) were computed at the B3LYP/6-31+G* level and were not scaled. All transition structures and minima were fully characterized by harmonic analysis. For each located transition structure, only one imaginary frequency was obtained in the diagonalized Hessian matrix, and the corresponding vibration was found to be associated with nuclear motion along the reaction coordinate under study. For the parent model reaction **1a** + **1a** → *p*-**2a** (see Scheme 2), intrinsic reaction coordinate (IRC)[19] calculations were performed

(14) Frisch, M. J.; Trucks, G. W.; Schlegel, H. B.; Scuseria, G. E.; Robb, M. A.; Cheeseman, J. R.; Zakrzewski, V. G.; Montgomery, J. A., Jr.; Stratmann, R. E.; Burant, J. C.; Dapprich, S.; Millam, J. M.; Daniels, A. D.; Kudin, K. N.; Strain, M. C.; Farkas, O.; Tomasi, J.; Barone, V.; Cossi, M.; Cammi, R.; Mennucci, B.; Pomelli, C.; Adamo, C.; Clifford, S.; Ochterski, J.; Petersson, G. A.; Ayala, P. Y.; Cui, Q.; Morokuma, K.; Malick, D. K.; Rabuck, A. D.; Raghavachari, K.; Foresman, J. B.; Cioslowski, J.; Ortiz, J. V.; Stefanov, B. B.; Liu, G.; Liashenko, A.; Piskorz, P.; Komaromi, I.; Gomperts, R.; Martin, R. L.; Fox, D. J.; Keith, T.; Al-Laham, M. A.; Peng, C. Y.; Nanayakkara, A.; Gonzalez, C.; Challacombe, M.; Gill, P. M. W.; Johnson, B.; Chen, W.; Wong, M. W.; Andres, J. L.; Gonzalez, C.; Head-Gordon, M.; Replogle, E. S.; Pople, J. A. *Gaussian 98*, revision A.5; Gaussian, Inc.: Pittsburgh, PA, 1998.

(15) Hehre, W. J.; Radom, L.; Schleyer, P. v. R.; Pople, J. A. *Ab Initio Molecular Orbital Theory*; Wiley: New York, 1986; pp 76–87 and references therein.

(16) Parr, R. G.; Yang, W. *Density-Functional Theory of Atoms and Molecules*; Oxford: New York, 1989.

(17) (a) Kohn, W.; Becke, A. D.; Parr, R. G. *J. Phys. Chem.* **1996**, *100*, 12974. (b) Becke, A. D. *J. Chem. Phys.* **1993**, *98*, 5648. (c) Becke, A. D. *Phys. Rev. A* **1988**, *38*, 3098.

(18) (a) Goldstein, E.; Beno, B.; Houk, K. N. *J. Am. Chem. Soc.* **1996**, *118*, 6036. (b) Wiest, O.; Montiel, D. C.; Houk, K. N. *J. Phys. Chem. A* **1997**, *101*, 8378. (c) García, J. I.; Martínez-Merino, V.; Mayoral, J. A.; Salvatella, L. *J. Am. Chem. Soc.* **1998**, *120*, 2415.

(19) Gonzalez, C.; Schlegel, H. B. *J. Phys. Chem.* **1990**, *94*, 5523.

to connect unambiguously the transition structure with the reactants and the corresponding cycloadduct.

Bond orders and atomic charges were calculated with the Natural Bond Orbital (NBO)[20] method.

The molecular hardness (η) of several species was computed according to the following approximate expression:[21]

$$\eta = \frac{1}{2}(\epsilon_L - \epsilon_H) \tag{1}$$

where ϵ_L and ϵ_H are the energies of the LUMO and HOMO, respectively.

Resonance integrals ($\beta_{i,j}$) between AOs were computed by means of the Mulliken approximation[22] according to the following equation:

$$\beta_{i,j} = \frac{1}{2}(\beta_i^o + \beta_j^o)S_{i,j} \tag{2}$$

where $S_{i,j}$ is the overlap integral between the AOs under consideration, and β_i^o and β_j^o are fixed parameters for the *i*- and *j*-atoms, respectively. We have used the parameters included in the AM1 Hamiltonian[23,24] for the carbon and boron elements. Thus, $\beta_C^{2p} = -0.28367$ au and $\beta_B^{2p} = -0.23055$ au.

The values of $S_{i,j}$ were computed according to the analytical expressions reported by Mulliken et al.[25] for the σ-overlap between two 2p AOs:

$$S_{CB} = \frac{p^5}{16}(1 - t^2)^{5/2}[A_2(B_0 + B_4) - B_2(A_0 + A_4)] \tag{3}$$

$$S_{CC} = \frac{p^5}{120}[5A_4 - 18A_2 + 5A_0] \tag{4}$$

where *t* and *p* are respectively

$$t = \frac{|\xi_i - \xi_j|}{\xi_i + \xi_j} \tag{5}$$

$$p = \frac{1}{2a_o}(\xi_i + \xi_j)R_{i,j} \tag{6}$$

In eqs 5 and 6, a_o is the Bohr radius, ξ_i and ξ_j being the Slater exponents of the corresponding atoms. We used the exponents reported by Dewar et al. for the carbon and boron elements.[23,24] Therefore, $\xi_C = 1.685116$ bohr^{-1} and $\xi_B = 1.555385$ bohr^{-1}. The A_K and B_K terms in eqs 3 and 4 were calculated as[25]
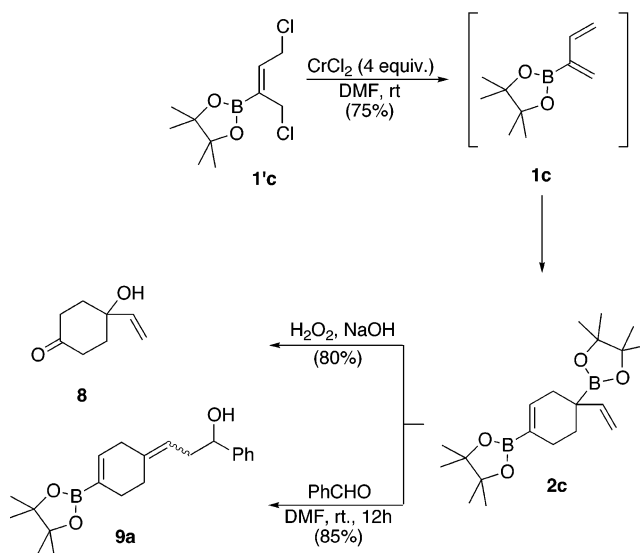
$$A_K = e^{-p}\sum_{\mu=1}^{k+1}\left[\frac{k!}{p^\mu(k - \mu + 1)!}\right] \tag{7}$$

$$B_K = -e^{-pt}\sum_{\mu=1}^{k+1}\left[\frac{k!}{(pt)^\mu(k - \mu + 1)!}\right] - e^{pt}\sum_{\mu=1}^{k+1}\left[\frac{(-1)^{k-\mu}k!}{(pt)^\mu(k - \mu + 1)!}\right] \tag{8}$$

Results and Discussion

The (1,3-butadien-2-yl)boronate **1c** can be obtained by reductive dechlorination of the pinacol ester of the (1,4-

SCHEME 3

dichloro-2-buten-2-yl)boronic acid **1'c** (Scheme 3) in the presence of a metal.[4b] We found that the use of 4 equiv of CrCl$_2$ in dry DMF at room temperature leads directly to the adduct **2c**, the result of dimerization of **1c**, in 75% yield. Analysis of the ^{1}H and ^{13}C NMR spectra of **2c** suggested the presence of only one regioisomer. To verify this hypothesis and to determine the exact structure of the dimer, oxidation of this compound was carried out with hydrogen peroxide in the presence of sodium hydroxide (Scheme 3). The product thus obtained with a good yield (80%) was unambiguously identified as being a symmetrical cyclohexanone, the 4-hydroxy-4-vinylcyclohexanone **8**.[26] This result suggests that the dimer **2c** arises from reaction of the more electron deficient dienophilic π-bond in **2** and results in para-selectivity.[27]

At this stage of our work, we envisioned that the new boron reagent **2c**, which contains an allylboronate functionality, could be used for further elaboration of six-membered rings. The dimer **2c** reacted smoothly with benzaldehyde at room temperature to give, after hydrolysis, the expected homoallylic alcohol **9a** in 85% yield. The ^{13}C NMR analysis of the crude reaction mixture indicated the formation of an ca. 1:1 mixture of stereoisomers with respect to the exocyclic double bond not containing the boron group (Scheme 3). To obtain directly the corresponding alcohols in only one step from the boronate **1'c**,

(20) (a) Reed, A. E.; Curtiss, L. A.; Weinhold, F. *Chem. Rev.* **1988**, *88*, 899. (b) Reed, A. E.; Weinstock, R. B.; Weinhold, F. *J. Chem. Phys.* **1985**, *83*, 735.

(21) (a) Parr, R. G.; Donelly, R. A.; Levy, M.; Palke, W. E. *J. Chem. Phys.* **1978**, *68*, 3801. (b) Parr, R. G.; Pearson, R. G. *J. Am. Chem. Soc.* **1983**, *105*, 7512. (c) Mulliken, R. S. *J. Chem. Phys.* **1934**, *2*, 782.

(22) (a) Mulliken, R. S. *J. Chem. Phys.* **1949**, *46*, 675. (b) Mulliken, R. S. *J. Chem. Phys.* **1952**, *56*, 295.

(23) Dewar, M. J. S.; Zoebisch, E. G.; Healy, E. F.; Stewart, J. J. P. *J. Am. Chem. Soc.* **1985**, *107*, 3902.
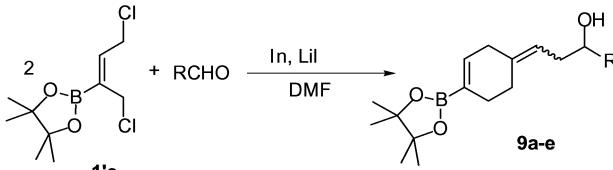
(24) Dewar, M. J. S.; Jie, C.; Zoebisch, E. G. *Organometallics* **1988**, *7*, 513.

(25) Mulliken, R. S.; Rieke, C. A.; Orloff, D.; Orloff, H. *J Chem. Phys.* **1949**, *17*, 1248.

(26) The structure was confirmed by the synthesis of **4** from the commercially available monoprotected cyclohexane-1,4-dione according to the procedure described in the following publication: Coogan, M. P.; Knight, D. W. *Tetrahedron Lett.* **1996**, *37*, 6417.

(27) It should be noted that the dimerization of the 2-carboxymethoxybutadiene gives the same regioselectivity. Spino, C.; Crawford, J.; Ciu, Y.; Gugelchuk, M. *J. Chem. Soc., Perkin Trans. 2* **1998**, 1499.

TABLE 1. Cyclic Products 1′c → 9a−e from Tandem Dimerization/Allylboration[a]

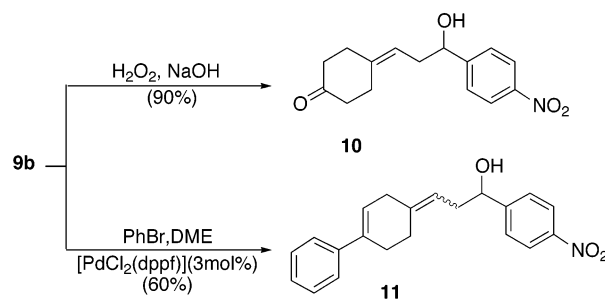| entry	aldehyde	product	yield (%)[b]
1	PhCHO	**9a**	78
2	4-NO$_2$C$_6$H$_4$−CHO	**9b**	65
3	3-NO$_2$C$_6$H$_4$−CHO	**9c**	71
4	*trans*-CH$_3$CH=CHCHO	**9d**	50
5	*n*-C$_5$H$_{11}$CHO	**9e**	55

[a] All reactions were carried out by heating a 2/1/1/1 mixture of boronate/indium/LiI/aldehyde in dry DMF [∼0.2 M] at 90 °C for 3 h. [b] Unoptimized yields of products isolated after flash chromatography purification. A ca. 1:1 mixture of *E* and *Z* olefins at the indicated position was obtained.

we thus tried to carry out the Diels−Alder dimerization in the presence of an aldehyde. After some unsuccessful experiments, it was found that **9a** can be obtained from **1′c** in the presence of benzaldehyde and chromium(II) chloride in DMF at 80 °C with an overall chemical yield of 45%. However, the use of indium metal instead of CrCl$_2$ significantly improved the yield. The optimized conditions required a 2/1/1/1 mixture of boronate/indium/LiI/aldehyde in DMF at 90 °C for 3 h (Table 1, entry 1). The reaction was examined with other aldehydes and the products **9b−d** resulting of this unprecedented tandem reaction were isolated in moderate to good yields (entries 2−5).[28] In light of the above results, the reaction should be generalizable with a wide variety of aldehydes, although the best yields were obtained with aromatic aldehydes. It is also worth noting that this simple one-pot procedure gives access to new cycloalkenylboronic esters which could not easily be prepared by other methods.

As is shown for **9b** used as a model compound, these boronates can be efficiently oxidized to the corresponding ketones **10** by using sodium hydroxide and hydrogen peroxide or coupled with an aryl halide in the presence of CsF and a catalytic amount of [PdCl$_2$(dppf)] in refluxing DME to furnish **11** (Scheme 4).

Once we had studied and optimized the conditions for the dimerization and functionalization of compounds **1**, we decided to study computationally the two model reactions included in Scheme 2, to unveil the reasons underlying the behavior of these compounds in the course of the cycloaddition step.

The thermal dimerization of boryl diene **1a** was studied first. According to our results, the transoid conformation of **1a** is 1.48 kcal/mol more stable than its cisoid conformer, at the B3LYP/6-31+G* level, the geometric

(28) For examples of tandem reactions involving Diels−Alder reaction followed by the condensation with an aldehyde, see: (a) Vaultier, M.; Truchet, F.; Carboni, B.; Hoffmann, R. W.; Denne, I. *Tetrahedron Lett.* **1987**, *28*, 4169. (b) Renard, P. Y.; Lallemand, J. Y. *Bull. Soc. Chim. Fr.* **1996**, *133*, 143. (c) Renard, P. Y.; Lallemand, J. Y. *Tetrahedron: Asymmetry* **1996**, *7*, 2523. (d) Renard, P. Y.; Six, Y.; Lallemand, J. Y. *Tetrahedron Lett.* **1997**, *38*, 6589. (e) Six, Y.; Lallemand, J. Y. *Tetrahedron Lett.* **1999**, *40*, 1295. (f) Tailor, J.; Hall, D. G. *Org. Lett.* **2000**, *2*, 3715.

SCHEME 4

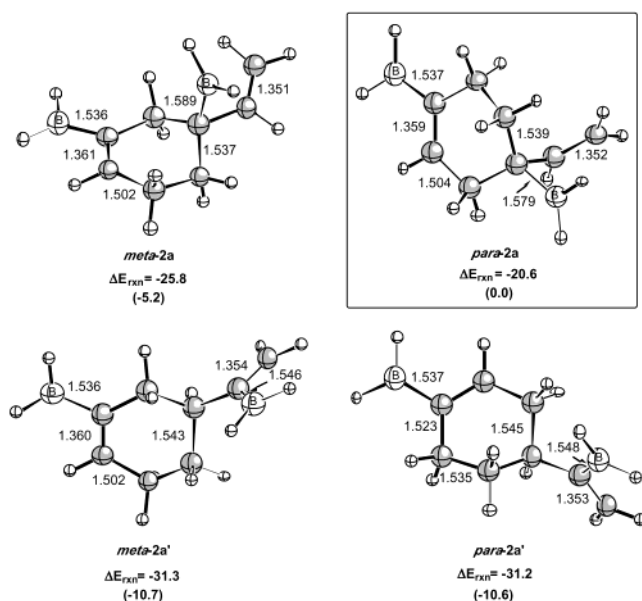features being quite normal for this kind of compound (Figure 1A).

In contrast with its apparent simplicity, **1a** can react in four different ways, as is shown in Scheme 2. The structures and relative energies of meta- and para-regioisomers **2a** and **2a′** are reported in Figure 2. According to our results, *m*-**2a′** is the most stable cycloadduct, whereas *p*-**2a** is the less stable one. Therefore, this latter compound, which corresponds to the experimentally observed regiochemistry, requires kinetic control to be obtained.

The frontier orbitals of 2-boryl-1,3-dienes are qualitatively different from those of normal 1,3-dienes. Thus, the HOMO of a 1,3-diene does not mix significantly with the unoccupied p-AO of the sp^2-hybridized boron atom. Instead, given the close proximity between the LUMO of the 1,3-diene and the p-AO of boron, the corresponding in-plane combination lowers the energy of the LUMO of the 2-boryl-1,3-diene, as can be seen in Figure 3. This results in a softer and more reactive molecule. Thus, the η values for the transoid conformers of 1,3-butadiene and
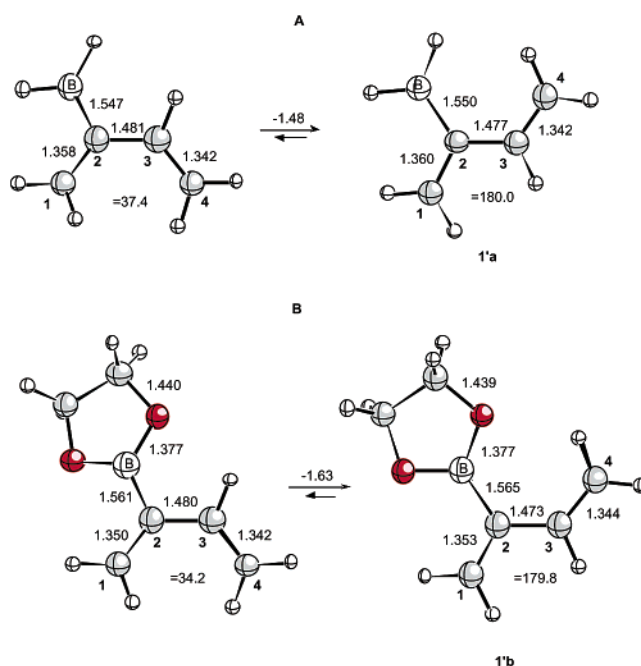

FIGURE 1. Fully optimized structures (B3LYP/6-31+G* level) of cisoid and transoid forms of dienes **1′a** and **1′b**. Bond distances and angles are given in Å and deg, respectively. Dihedral angles $\omega = C_1-C_2-C_3-C_4$ are in absolute value. Numbers over the arrows are the energies in kcal/mol (B3LYP/6-31+G*+ΔZPVE level) associated with the cisoid−transoid conformational transformation.

FIGURE 2. B3LYP/6-31+G* optimized geometries of the posible cycloadducts corresponding to the dimerization of **1a** (see Scheme 2, reaction 1). Bond distances are given in Å. ΔE_{rxn} values denote the relative energies in kcal/mol with respect to 2 equiv of **1a**. Bold numbers are the reaction energies (in kcal/mol) with respect to the separate reagents. Numbers in parentheses are the relative energies in kcal/mol (B3LYP/6-31+G*+ΔZPVE level) with respect to *p*-**2a**, which corresponds to the regiochemistry observed experimentally.
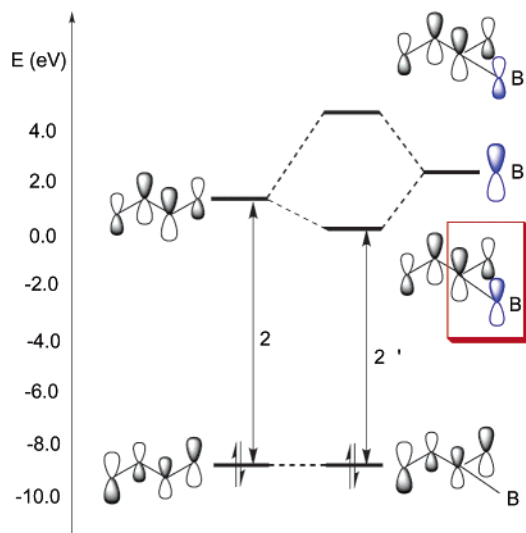
FIGURE 3. Schematic representation of the FMOs of a general 1,3-diene and a 2-boryl-1,3-diene. η is the molecular hardness of the corresponding species.

1′a are calculated to be 0.09966 and 0.08329 au, respectively, at the B3LYP/6-31+G* level. Therefore, **1a** is a more active dienophile than normal 1,3-butadienes. In addition, the topology of the LUMO of **1a** allows for three modes of interaction with the diene: a "normal" [4+2] interaction that leads to the formation of the C_1–C_1 and C_4–$C_{2'}$ bonds (Figure 4) and a [4+3] interaction in which the C_1–$C_{1'}$ and C_4–$B_{5'}$ bonds are formed. The third interaction mode consists of the [4+2] interaction involving the double bond between $C_{3'}$ and $C_{4'}$.
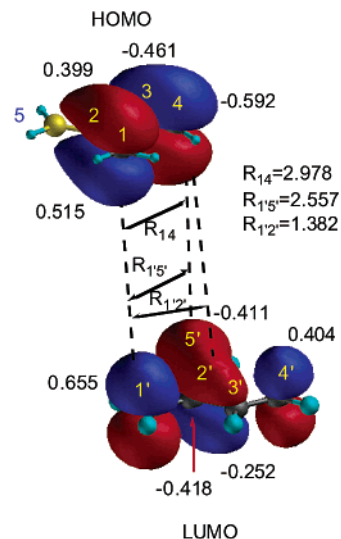

FIGURE 4. AM1 representation of the FMOs of **1′a**. Numbers correspond to the expansion coefficients. Only the *para-endo* (see Figures 5 and 6) geometry leading to **TS1** has been included. Interatomic distances are given in Å.

However, the LUMO expansion coefficients of the $C_{3'}$ and $C_{4'}$ terms are significantly lower than those corresponding to $C_{1'}$ and $C_{2'}$ (Figure 4), thus suggesting that the double bond closer to the boron atom is more reactive in a thermal cycloaddition.

As we have mentioned before (Scheme 2), dimerization of **1a** has two possible regiochemistries according to the relative position of both BH_2 groups. We have denoted *meta* and *para* those regioisomers in which both BH_2 groups are separated by three or four carbon atoms, respectively. In both regioisomers, two possible stereochemistries can be envisaged, which correspond to [4+2] or [4+3] transition structures in which the boron atom occupies the *endo* and *exo* positions, respectively. Finally, two cisoid and transoid conformations are possible for each transition structure, thus yielding eight possible transition structures (Figure 5).

We have computed these saddle points and the chief and relative energies of transition structures **TS1–16** are reported in Figure 6 and in Figures S1–S3 of the Supporting Information. In good agreement with the experimental findings, transition structures leading to *p*-**2a** are of lower energy than those associated with formation of the remaining cycloadducts. This indicates that formation of *p*-**2a** is favored under kinetic control. For the *para*-transition structures **TS1** and **TS3**, the *endo* or *exo* disposition of the "dienophilic" boron atom results in almost isoenergetic saddle points. In contrast, the analogue *meta-endo* transition structures are significantly less energetic than the corresponding exo *congener* (Figure S1). As expected, transition structures **TS11–18** (Figures S2 and S3), associated with reaction through the double bond between the $C_{3'}$ and $C_{4'}$ atoms, are of much larger energy than those reported in Figures 6 and S1. The exception is **TS14**, which is ca. 3.5 kcal/mol lower in energy than the related transition structures. This relative stabilization is due to a partial bonding between one hydrogen atom of the BH_2 group and the other boron atom (Figure S3). Since the experimental study involves
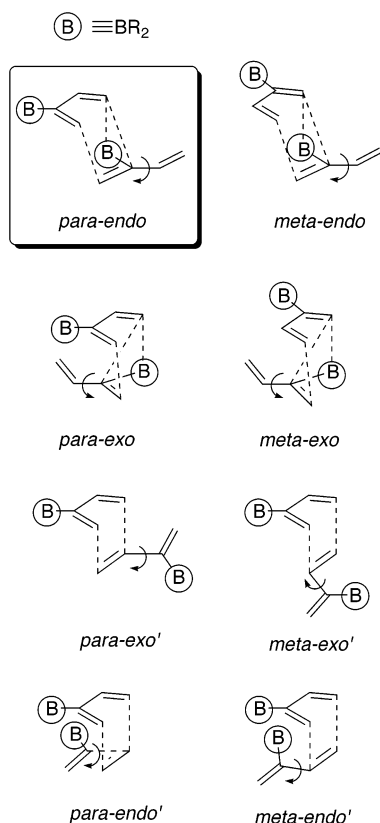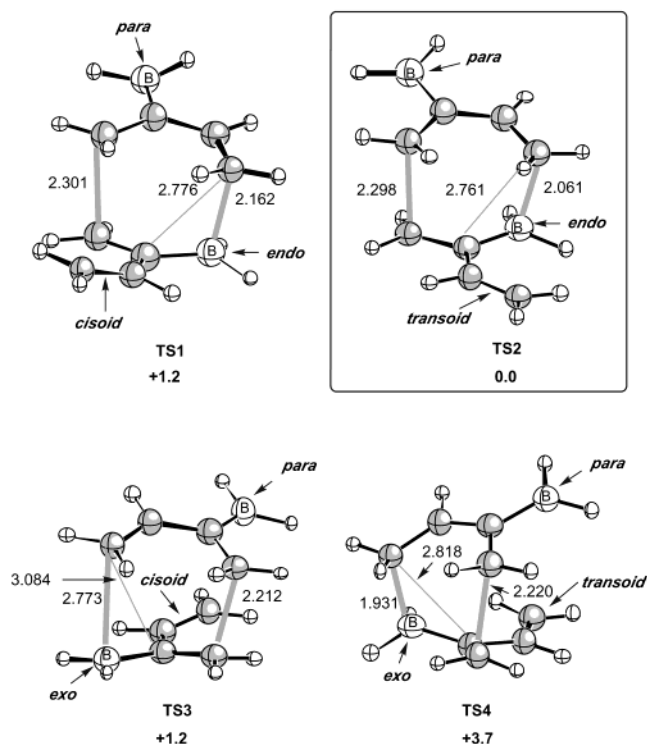
FIGURE 5. Schematic representation of the possible regio- and stereochemistries in the dimerization of 2-boryl(boronyl)-1,3-dienes. For each structure, the presence of cisoid and transoid conformers is indicated by means of a curved arrow.

FIGURE 6. B3LYP/6-31+G* fully optimized geometries of transition structures **TS1−4** associated with the dimerization of **1a** to form *p*-**2a** (see Scheme 2, reaction 1). Bond distances are given in Å. Bold numbers are the relative energies (in kcal/mol) with respect to **TS2**.

B−O bonds, this partial stabilization is not relevant from an experimental standpoint.

According to our results, **TS2** is the less energetic transition structure (Figure 6). In this saddle point, both BH$_2$ groups are *para* to each other, and the boron atom associated with the [4+3] geometry is in an *endo* disposition, the exocyclic double bond being in a transoid conformation. Therefore, the activation energy associated with reaction 1 of Scheme 2 is found to be of only ca. 7.5 kcal/mol at the B3LYP/6-31+G*+ΔZPVE level. The [4+3] character of transition structures reported in Figure 6 is remarkable, with C$_1$···C$_{1'}$ and C$_4$···B$_{5'}$ distances of ca. 2.3 and 2.1 Å, respectively, the C$_4$···C$_{2'}$ distances being significantly larger. These results are in line with those reported by Singleton[10a] for the reaction between 1,3-butadiene and borylethylene. In contrast, de Pascual-Teresa and Houk[29] have reported that the ionic Diels−Alder reaction between allyl cation and 1,3-butadiene is stepwise.

The [4+3] approach between the two molecules of **1a** can be understood in terms of the appropriate symmetry of the corresponding FMOs (Figure 4). In addition, the C$_{1'}$−C$_{5'}$ distance is larger than that between C$_{1'}$ and C$_{2'}$ atoms and is therefore closer to the C$_1$−C$_4$ distance. This means that the overlap required for the [4+3] interaction is favored over that required for the [4+2] approach, since it demands a lower distortion of the reactants. On the

other hand, according to second-order perturbation theory,[30] the stabilizing term associated with two-electron interactions between two molecules of **1a** can be approximated as

$$\Delta E_{2e} \approx \frac{-1}{\eta}\{[c_1^H c_{1'}^L \beta_{1,1'} + c_4^H (c_{5'}^L \beta_{4,5'} + c_{2'}^L \beta_{4,2'})]^2 + (c_1^L c_{1'}^H \beta_{1,1'} + c_4^L c_{2'}^H \beta_{4,2'})^2\} \quad (9)$$

In this expression, η is the hardness of **1a**, c_i^H and c_j^L are the HOMO and LUMO coefficients of i and j atoms, respectively, and $\beta_{i,j}$ values are the corresponding resonance integrals. Inspection of eq 9 reveals that, because of the nonmixing of the p AO of boron in the HOMO, there are two terms corresponding to the [4+2] pathway, whereas there is only one associated with the [4+3] approach, the remaining terms being common for both channels. We can also define similar expressions for "pure" [4+3] and [4+2] processes according to eqs 10 and 11:

$$\Delta E_{[4+3]} \approx \frac{-1}{\eta}[(c_1^H c_{1'}^L \beta_{1,1'} + c_4^H c_{5'}^L \beta_{4,5'})^2 + (c_1^L c_{1'}^H \beta_{1,1'})^2] \quad (10)$$

$$\Delta E_{[4+2]} \approx \frac{-1}{\eta}[(c_1^H c_{1'}^L \beta_{1,1'} + c_4^H c_{2'}^L \beta_{4,2'})^2 + (c_1^L c_{1'}^H \beta_{1,1'} + c_4^L c_{2'}^H \beta_{4,2'})^2] \quad (11)$$

(29) de Pascual-Teresa, B.; Houk, K. N. *Tetrahedron Lett.* **1996**, *37*, 1759.

(30) (a) Salem, L. *J. Am. Chem. Soc.* **1968**, *90*, 223. (b) Salem, L. *J. Am. Chem. Soc.* **1968**, *90*, 543.
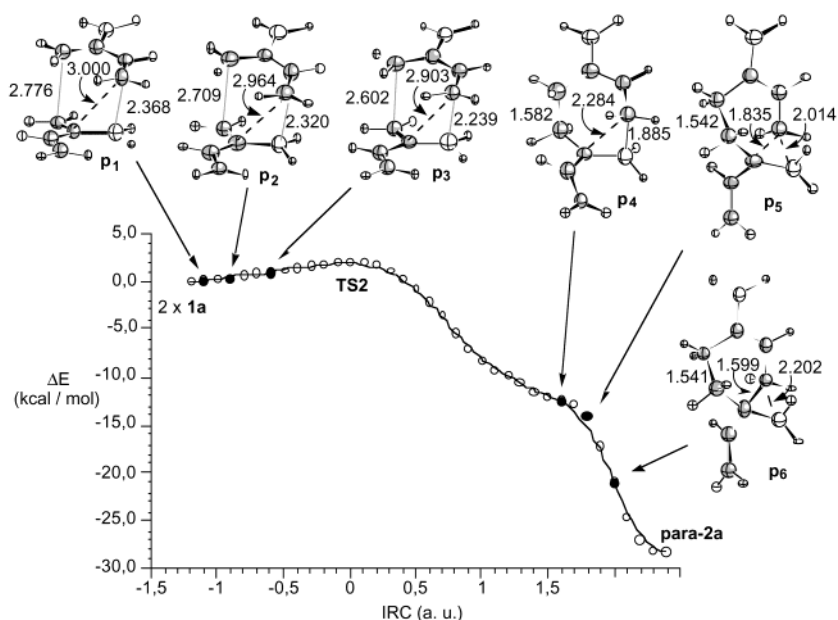
FIGURE 7. Intrinsic Reaction coordinate plot (IRC) of reaction 1, performed at the B3LYP/6-31G* level. The figure includes the geometries of selected points along the IRC. Bond distances are given in Å. Points beyond **p$_4$** do not correspond to the IRC, but are intermediate points obtained in the course of the optimization of **p$_4$**, which spontaneously converged to *p*-**2a**.
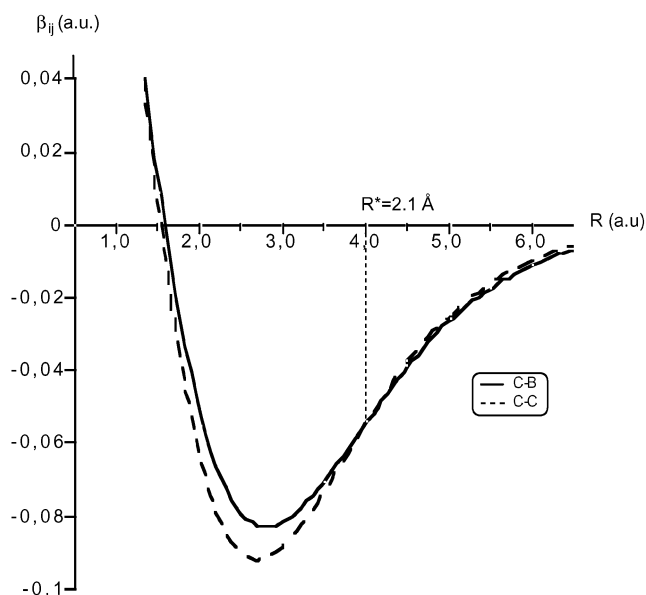
TABLE 2. Overlap Integrals ($S_{i,j}$),[a] Resonance Integrals ($\beta_{i,j}$, kcal/mol),[b] Two-Electron Interaction Energies (ΔE_{2e}, kcal/mol),[c] [4+3] Interaction Energies ($\Delta E_{[4+3]}$, kcal/mol),[d] and [4+2] Interaction Energies ($\Delta E_{[4+2]}$, kcal/mol)[e] Computed for Points p$_1$–p$_3$[f]

	p$_1$	**p$_2$**	**p$_3$**
$S_{1,1'}$	0.068	0.077	0.092
$S_{4,2'}$	0.046	0.049	0.055
$S_{4,5'}$	0.153	0.164	0.182
$\beta_{1,1'}$	−12.19	−13.71	−16.45
$\beta_{4,2'}$	−8.10	−8.67	−9.70
$\beta_{4,5'}$	−24.74	−26.39	−29.35
ΔE_{2e}	−3.38	−4.02	−5.32
$\Delta E_{[4+3]}$	−2.29	−2.74	−3.67
$\Delta E_{[4+2]}$	−0.65	−0.82	−1.17

[a] Computed by means of eqs 3−8. [b] Computed by means of eq 2. [c] Computed by means of eq 9. [d] Computed by means of eq 10. [e] Computed by means of eq 11. [f] See Figure 6 for the geometrical features of points **p$_1$**−**p$_3$**.

We have computed the [4+3] and [4+2] contributions at different points of the IRC plot reported in Figure 7, and the more significant data are collected in Table 2. According to these results, the contribution of the [4+2] terms is lower than that of the [4+3] approach at the initial stages of the **1a** + **1a** → *p*-**2a** reaction. This preference is caused by the smaller C$_4$−B$_{5'}$ distances in points **p$_1$**−**p$_3$** and the larger negative values of the corresponding resonance integrals (vide infra).

The remaining question is why *p*-**2a** instead of the corresponding [4+3] cycloadduct is formed. To solve this problem we have performed IRC calculations for the **1a** + **1a** → *p*-**2a** reaction starting from **TS2**. Our computations led to a zwitterionic structure **p$_4$** whose optimization collapsed to **2a** without any activation barrier (see Figure 7). Inclusion of solvent effects by means of self-consistent reaction field calculations (Onsager model[31]) led to the
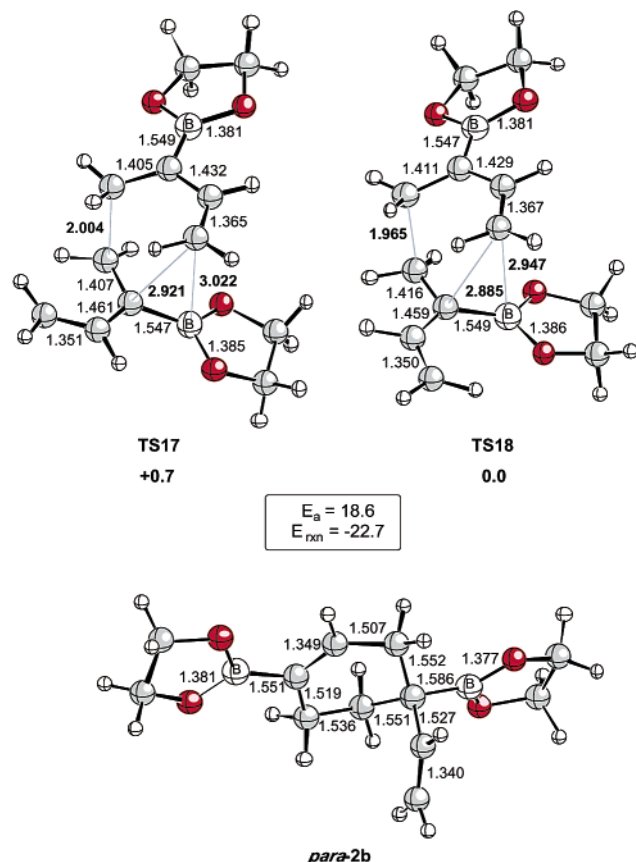
(31) (a) Onsager, L. *J. Am. Chem. Soc.* **1936**, *58*, 1486. (b) Wong, M. W.; Wiberg, K. B.; Frisch, M. J. *J. Am. Chem. Soc.* **1992**, *114*, 523.

FIGURE 8. Plot of the resonance integrals associated with σ-overlap between 2p AOs leading to the formation of C−C and C−B bonds. The R* point is the internuclear distance corresponding to the intersection between both curves.

same result and the zwitterionic intermediate associated with **p$_4$** could not be characterized. According to our results, **p$_4$** rearranges to *p*-**2a** by breaking the C$_4$−C$_{5'}$ bond and forming the final C$_4$−C$_{2'}$ σ bond both in the gas phase and in solution. This process can be appreciated by inspection of the geometric features of points **p$_5$** an **p$_6$** (Figure 7). One explanation for this behavior can be found if the resonance integrals associated with the σ-overlap between 2p AOs leading to a C−C or a C−B bond are computed at different internuclear distances (Figure 8). From our data calculated by means of eps 2−8 at large distances the resonance integral associated with

FIGURE 9. Fully optimized structures (B3LYP/6-31+G* level) of **TS17** and **TS18** associated with formation of *p*-**2b** from **1b**. Bond distances and angles are given in Å and deg, respectively. Bold number are the relative energies in kcal/mol (B3LYP/6-31+G*+ΔZPVE level) between the transoid and the cisoid TSs. The ΔE_a and ΔE_{rxn} values are the activation and reaction energies in kcal/mol (B3LYP/6-31+G*+ΔZPVE level) of the **1b** → *p*-**2b** model reaction.

formation of the C−B bond is more stabilizing than that corresponding to the C−C bond formation. This clearly favors the [4+3] approach, as it is found in the IRC study and in the geometry of **TS1**. However, beyond the R^* point (see Figure 8), the relative stabilities induced by both types of resonance integrals are in a reverse relationship, namely the C⋯C interaction is now *more* stabilizing than the C⋯B interaction. Interestingly, the crossing point is $R^* \approx 2.1$ Å, which corresponds approximately to the $C_4 \cdots B_{5'}$ bond distance in **TS2**. This means that beyond this saddle point formation of *p*-**2a** is progressively more favored than formation of the zwitterionic [4+3] cycloadduct **p4**.

We have also investigated computationally reaction 2, in which the 1,3-dioxolane moiety reproduces the system studied experimentally. The transoid form of **1b** is also slightly more stable than the corresponding cisoid conformer, as it is shown in Figure 1B. The two possible *para-endo* transition structures **TS17** and **TS18** are reported in Figure 9. We have found that the cisoid transition structure **TS17** is ca. 0.7 kcal/mol less stable than **TS18**. In the case of these transition structures, however, the $C_2 \cdots B_{5'}$ distances are larger than those calculated for the analogue saddle points calculated for reaction 1 (see Figure 6). This is due to the donating effect

of the oxygen atoms on the nonhybridized p AO of $B_{5'}$, as is shown by the NBO analysis of **TS18**. In addition, **TS18** has a larger [4+2] character than that observed in its analogue **TS2**. Thus, the $C4 \cdots B5'$ bond order for **TS18** is 0.050, whereas in the case of **TS2** the corresponding bond order is 0.387. In contrast, the $C4 \cdots C2'$ bond orders for **TS2** and **TS18** are 0.062 and 0.149, respectively. Therefore, the [4+3] vs [4+2] character of the transition structures associated with this kind of reaction is strongly affected by the nature of the boryl group. This results in a less efficient dipolarophile and consequently in a larger activation energy, the energy of reaction being quite similar to that of the **1a** + **1a** → *p*-**2a** reaction (Figure 9).

Conclusions

We have developed a novel tandem reaction for the concise construction of cyclic alkenylboronates based on the Diels−Alder dimerization of (1,3-butadien-2-yl)boronate followed by the condensation with an aldehyde. The computational study performed on the thermal cycloaddition of 2-boryl-1,3-butadienes helps to understand the reasons underlying the easy dimerization of these compounds under thermal conditions. The interaction of the nonhybridized p AO of boron with the LUMO of 1,3-butadiene results in a more active dipolarophile and in a new LUMO in which both the [4+2] and [4+3] processes are symmetry allowed. Analysis of the C−C and C−B resonance integrals, together with second order perturbation theory, shows that in the early stages of the reaction both approaches are compatible. In addition, the [4+3] pathway predominates in the initial stages of the reaction profile, because of the larger contribution of the C−B resonance integral. Beyond a distance of ca. 2.1 Å, the [4+2] mechanism is preferred and the hypothetical [4+3] zwitterionic intermediate collapses to the [4+2] cycloadduct without any activation barrier. The regiochemistry of these cycloadducts is in full agreement with that found experimentally.

Experimental Section

General Procedures. Unless otherwise specified, all reactions were performed in oven-dried glassware under an argon atmosphere. All chemical reagents were used as received unless otherwise indicated. All solvents indicated "dry" were dried by distillation. NMR spectra were recorded on a 200- or 300-MHz spectrometer operating in the Fourier transform mode. ^{13}C NMR spectra were obtained with broadband proton decoupling. Chemical shifts were recorded relative to the internal TMS (tetramethylsilane) reference signal. For ^{11}B NMR, the chemical shifts are in ppm relative to $BF_3 \cdot OEt_2$. Microanalyses were done at the Central Laboratory for Analysis, CNRS, Lyon, France. Silica gel 60F254 was used for column chromatography.

4,4,5,5-Tetramethyl-2-[4-(4,4,5,5-tetramethyl-1,3,2-dioxoborolan-2-yl)-1-vinylcyclohex-3-en-1-yl]-1,3,2-dioxaborolane (2c). To a stirred solution of chromium(II) chloride (2 g, 16.28 mmol, 4.0 equiv) in dry DMF (30 mL) was added the boronate **1′c** (1 g, 3.98 mmol, 1.0 equiv). After being stirred at room temperature for 16 h, the reaction mixture was quenched with water (10 mL). After additional stirring for 10 min, the resulting green solution was extracted with ethyl acetate (3 × 30 mL). The combined organic extracts were washed with water and brine, dried over $MgSO_4$, and concentrated in vacuo. The residue was purified by chromatography on silica gel (10%

ethyl acetate in heptane) to afford **2c** as a colorless solid (1.07 g, 2.97 mmol, 75%). TLC (50% ethyl acetate in heptane) R_f 0.60; mp 114−115°C. ^{1}H NMR (C_6D_6, 200 MHz) δ 7.08 (m, 1H), 6.04 (dd, $J = 17.5$, 10.6 Hz, 1H), 5.11 (dd, $J = 17.5$, 1.4 Hz, 1H), 5.04 (dd, $J = 10.6$, 1.4 Hz, 1H), 2.86−2.51 (m, 3H), 2.34−2.07 (m, 2H), 1.64 (m, 1H), 1.09 (s, 12H), 1.00 (s, 12H); ^{13}C NMR (CDCl$_3$, 50 MHz) δ 143.0, 141.3, 110.9, 82.2, 81.9, 32.2, 28.3, 23.7, 23.4. Anal. Calcd for $C_{20}H_{34}B_2O_4$: C, 66.71; H, 9.52; O, 17.77. Found: C, 66.59; H, 9.23; O, 17.72.

4-Hydroxy-4-vinylcyclohexanone (8). To a solution of dimer **2c** (256 mg, 0.71 mmol) in 2 mL of THF and 250 mL of sodium hydroxide (3 M) was added hydrogen peroxide (290 mL, 30%) at 0 °C. The solution was allowed warm to room temperature, maintained for 18 h, and partially concentrated under reduced pressure to remove THF. The aqueous solution was extracted with ether (2 × 10 mL). The combined organic phase was washed with ammonium chloride (10 mL), dried over magnesium sulfate, and concentrated in vacuo. The residue was purified by chromatography on silica gel (40% ethyl acetate in heptane) to afford **8** as a colorless oil (80 mg, 0.57 mmol, 80%). TLC (40% ethyl acetate in hexanes) R_f 0.20; ^{1}H NMR (CDCl$_3$, 200 MHz) δ 5.98 (dd, $J = 17.4$, 10.7 Hz, 1H), 5.30 (d, $J = 17.4$ Hz, 1H), 5.10 (d, $J = 10.7$ Hz, 1H), 2.72 (m, 2H), 2.20 (m, 2H), 2.00−1.85 (m, 5H); ^{13}C NMR (CDCl$_3$, 50 MHz) δ 210.8, 143.1, 112.0, 69.5, 29.3, 23.8, 23.5. Anal. Calcd for $C_8H_{12}O_2$: C, 68.55; H, 8.63; O, 22.83. Found: C, 68.67; H, 8.72; O, 22.89.

General Procedure for the Synthesis of Cycloalkenylboronic Esters (9a−e). To a stirred solution of boronate 1′ (251 mg, 1 mmol) and indium powder (57 mg, 0.5 mmol) in dry DMF (2.5 mL) was added lithium iodide (67 mg, 0.5 mmol) as a solid in one portion. After 2 min, aldehyde (0.5 mmol) was added dropwise via syringe. The solution was stirred at 90 °C until no aldehyde was detected by TLC analysis. Dichloromethane (20 mL) and water (5 mL) were added, and stirring was maintained at room temperature for 30 min. The layers were separated and the aqueous phase extracted with dichloromethane (2 × 10 mL). The combined organic layers were dried over magnesium sulfate and concentrated under reduced pressure. Purification was accomplished by flash chromatography on silica gel (elution with heptane−ethyl acetate). The *E*- and *Z*-isomers could not be separate during the purification.

4-[3-Hydroxy-3-(4-nitrophenyl)propylidene]cyclohexanone (10). To a solution of **9b** (200 mg, 0.52 mmol) in 2 mL of THF and 180 mL of sodium hydroxide (3 M) was added hydrogen peroxide (210 mL, 30%) at 0 °C. The solution was allowed warm to room temperature, maintained for 18 h, and partially concentrated under reduced pressure to remove THF.

The aqueous solution was extracted with ether (2 × 10 mL). The combined organic phase was washed with ammonium chloride (10 mL), dried over magnesium sulfate, and concentrated in vacuo. The residue was purified by chromatography on silica gel (50% ethyl acetate in heptane) to afford **10** as a colorless oil (129 mg, 0.47 mmol, 90%). TLC (50% ethyl acetate in heptane) R_f 0.42; ^{1}H NMR (CDCl$_3$, 200 MHz) δ 8.14 (d, $J = 8.7$ Hz, 2H), 7.48 (d, $J = 8.7$ Hz, 2H), 5.32 (m, 1H), 4.81 (t, $J = 6.3$ Hz, 1H), 2.23 (m, 11H); ^{13}C NMR (CDCl$_3$, 50 MHz) δ 210.1, 150.3, 146.3, 137.6, 125.6, 122.6, 118.5, 71.9, 40.5, 39.5, 36.7, 33.1, 25.3. Anal. Calcd for $C_{15}H_{17}NO_4$: C, 65.44; H, 6.22; O, 23.25. Found: C, 65.49; H, 6.28; O, 23.28.

1-(4-Nitrophenyl)-3-(4-phenylcyclohex-3-en-1-ylidene)-propan-1-ol (11). The vinylboronate **9b** (200 mg, 0.52 mmol) was suspended in DME (8 mL). Phenylbromide (54.8 mL, 0.52 mmol) and PdCl$_2$(dppf) (16 mmol) were added. The mixture was degassed and then heated at reflux under argon for 24 h. After cooling to room temperature, the mixture was partially concentrated, diluted with EtOAc (10 mL), and washed with water (10 mL). The aqueous layer was extracted with EtOAc (3 × 10 mL) and the combined organic extracts were dried (MgSO$_4$), filtered, and concentrated in vacuo. Chromatography on silica gel (EtOAc/heptane) then afforded the product **11** as a colorless oil (104.6 mg, 0.31 mmol, 60%). TLC (50% ethyl acetate in heptane) R_f 0.55; ^{1}H NMR (CDCl$_3$, 200 MHz) δ 8.12 (d, $J = 8.1$ Hz, 2H), 7.52−7.25 (m, 7H), 6.42 (m, 0.5H), 6.36 (m, 0.5H), 5.25 (m, 1H), 4.76 (m, 1H), 2.78 (m, 1H), 2.70 (m, 1H), 2.45 (m, 2H), 2.25−2.02 (m, 5H); ^{13}C NMR (CDCl$_3$, 50 MHz) δ150.4, 146.2, 145.7, 140.6, 139.9, 139.7, 139.5, 138.6, 125.6, 125.2, 122.5, 65.1, 36.7, 36.2, 35.9, 32.1, 28.8, 27.5, 27.4, 24.6. Anal. Calcd for $C_{21}H_{21}NO_3$: C, 75.20; H, 6.31; O, 14.31. Found: C, 75.30; H, 6.36; O, 14.35.

Supporting Information Available: Total energies (au) and ZPVEs (au) and Cartesian coordinates of all the stationary points discussed in this work; main geometric features of transition structures **TS5**−**TS16** and relative energies of these saddle points with respect to **TTS2** (kcal/mol); characterization data for compounds **9a**−**e**. This material is available free of charge via the Internet at http://pubs.acs.org.

JO026491I